

α -Conotoxins ImI and ImII Target Distinct Regions of the Human $\alpha 7$ Nicotinic Acetylcholine Receptor and Distinguish Human Nicotinic Receptor Subtypes[†]

Michael Ellison,^{*,‡} Fan Gao,[§] Hai-Long Wang,[§] Steven M. Sine,[§] J. Michael McIntosh,^{‡,||} and Baldomero M. Olivera[‡]

Departments of Biology and Psychiatry, University of Utah, Salt Lake City, Utah 84112, and Receptor Biology Laboratory, Department of Physiology and Biomedical Engineering, Mayo Clinic College of Medicine, Rochester, Minnesota 55905

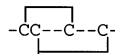
Received May 26, 2004; Revised Manuscript Received October 5, 2004

ABSTRACT: The *Conus* peptides α -conotoxin ImI (α -ImI) and ImII (α -ImII) differ by only three of 11 residues in their primary sequences and yet are shown to inhibit the human $\alpha 7$ nicotinic acetylcholine receptor (nAChR) by targeting different sites. Mutations at both faces of the classical ligand binding site of the $\alpha 7$ nAChR strongly affect antagonism by α -ImI but not α -ImII. The effects of the mutations on α -ImI binding and functional antagonism are explained by computational docking of the NMR structure of α -ImI to a homology model of the ligand binding domain of the $\alpha 7$ nAChR. A distinct binding site for α -ImII is further demonstrated by its weakened antagonism for a chimeric receptor in which the membrane-spanning domains and intervening linkers of the $\alpha 7$ nAChR are replaced with the corresponding sequence from the serotonin type-3 receptor (5HT₃). The two toxins also discriminate between different subtypes of human nicotinic receptors; α -ImII most strongly blocks the human $\alpha 7$ and $\alpha 1\beta 1\delta\epsilon$ receptor subtypes, while α -ImI most potently blocks the human $\alpha 3\beta 2$ subtype. Collectively, the data show that while α -ImI targets the classical competitive ligand binding site in a subtype selective manner, α -ImII is a probe of a novel inhibitory site in homomeric $\alpha 7$ nAChRs.

Nicotinic acetylcholine receptors (nAChRs)¹ are ACh-gated ion channels. Each receptor is a pentamer of subunits organized around a central ion-conducting pore. ACh binds to these receptors at the classical ligand binding site in a cleft formed at the interface between adjacent subunits. There are many different nAChR subunits ($\alpha 1$ – $\alpha 10$, $\beta 1$ – $\beta 4$, δ , ϵ , and γ), and these can associate in various combinations to form functional pentameric complexes, resulting in a large number of nAChR subtypes. The subtypes include homomers such as $\alpha 7$, heteromers with two different types of subunit (e.g., $\alpha 3\beta 2$), or more complex heteromers such as the muscle subtype, $\alpha 1\beta 1\delta\epsilon$ (1).

The nAChR subunits and the subunit of the homopentameric serotonin type-3 receptor (5HT₃) are highly conserved and share the same transmembrane topology. These subunits all have a large extracellular N-terminal domain where ACh or serotonin binds (the ligand binding domain). This domain is followed by four transmembrane regions and the associated extracellular loop, two intracellular loops, and the C-terminal extracellular tail (2); the transmembrane regions are numbered M1–M4 in the N- to C-terminal

Table 1: Characteristic Disulfide Scaffold of α -Conotoxins and Primary Structures of α -ImI and α -ImII^a

The primary structures of α -ImI and α -ImII	
α -ImI	GCCSDPRCAWRC*
α -ImII	ACCSDRRCRWRC*
The α -conotoxin disulfide scaffold	
	

^a The asterisk indicates C-terminal amidation. For α -ImII, the disulfide connectivity of the native peptide has not been confirmed but is assumed to be the same as that of α -ImI (5).

direction. Functional ACh-gated chimeric receptors can be made with the $\alpha 7$ nAChR N-terminal domain and the rest of the molecule from the 5HT₃ receptor (3).

Subtype-specific ligands and inhibitors are potentially useful tools for studying nAChRs, determining their normal physiological roles, and assessing their involvement in specific pathological states. The α -conotoxin family of disulfide-bonded peptides, from the venoms of the approximately 500 species of cone snails (*Conus*), is a potentially rich source of such antagonists (4). α -Conotoxins have a characteristic cysteine arrangement and connectivity (Table 1). $\alpha 4/3$ -Conotoxins are a subfamily of α -conotoxins characterized by four amino acid residues in their first inter-cysteine loop and three in their second loop. The first $\alpha 4/3$ -conotoxin to be described was α -conotoxin ImI (α -ImI) from *Conus imperialis*; it was found to block homomeric $\alpha 7$ and $\alpha 9$ nAChRs (5). Subsequently, the gene sequence (but not the native peptide from venom) of a second $\alpha 4/3$ -conotoxin, α -conotoxin ImII (α -ImII), was identified in *C.*

[†] This work was supported by National Institutes of Health Grants GM48677 (B.M.O.), MH53631 (J.M.M.), and NS31744 (S.M.S.).

* To whom correspondence should be addressed: Department of Biology, University of Utah, 257 S. 1400 East, Salt Lake City, UT 84112. Telephone: (801) 581-8370. Fax: (801) 585-5010. E-mail: michael.ellison@m.cc.utah.edu.

[‡] Department of Biology, University of Utah.

[§] Mayo Clinic College of Medicine.

^{||} Department of Psychiatry, University of Utah.

¹ Abbreviations: 5HT₃ receptor, serotonin type-3 receptor; α -ImI, α -conotoxin ImI; α -ImII, α -conotoxin ImII; ACh, acetylcholine; nAChR, nicotinic acetylcholine receptor; $\alpha 7$ receptor or $\alpha 7$ nAChR, $\alpha 7$ nicotinic acetylcholine receptor.

imperialis. Synthetic α -ImII also inhibits the $\alpha 7$ nAChR but, on the basis of competition studies, seems to bind to a different site on the receptor (6).

To further explore the α -ImI and α -ImII binding sites, we measured the abilities of the toxins to functionally inhibit $\alpha 7/5HT_3$ chimeric receptors (the nicotinic portion of which was human) with mutations at either the principal or complementary faces of the ligand binding site, and performed computational docking of α -ImI to a homology model of the major extracellular domain of the $\alpha 7$ nAChR. We also further characterized the subtype specificities of these peptides.

MATERIALS AND METHODS

Conotoxin Synthesis. Linear α -ImI and α -ImII were synthesized by standard Fmoc [*N*-(9-fluorenyl)methoxycarbonyl] chemistry, using an ABI model 430A peptide synthesizer at a University of Utah core facility. As described previously (7), linear peptides were cleaved from solid-phase synthesis resin and were oxidized using an orthogonal Cys protection strategy to give the correct disulfide connectivity (see Table 1). Coelution with native peptide was used to ensure that synthetic α -ImI was equivalent to the native peptide (data not shown). The α -ImII connectivity was assumed to be the same as that of α -ImI (Table 1).

Mutagenesis. An $\alpha 7$ nAChR clone in pRBG4 (8, 9) was mutated to a Q117S variant using the QuickChange kit (Stratagene, La Jolla, CA). Mutation was also introduced to alter those regions of an $\alpha 7/5HT_3$ chimera (8, 9) that are extracellular and also composed of the $5HT_3$ sequence. These regions were delineated using the predicted extracellular regions of the mouse $5HT_3$ subunit (2), and pairwise BLAST alignment of this protein with the $\alpha 7$ nAChR subunit. The three regions defined in this way were (1) the extracellular loop between transmembrane regions M2 and M3, (2) the C-terminal extracellular tail, and (3) the five residues in the N-terminal extracellular domain just to the N-terminal side of transmembrane region M1. PCR primers with nonannealing portions composed of $\alpha 7$ sequence that replaces corresponding $5HT_3$ sequence were used to amplify mutated and overlapping fragments of the $\alpha 7/5HT_3$ clone. By using natural and mutagenically introduced restriction sites, the mutated fragments were used to replace the corresponding parts of the original $\alpha 7/5HT_3$ clone. In this way, the loop and tail of the chimera (as well as both simultaneously) were converted from $5HT_3$ sequence to $\alpha 7$ sequence. Also, the five residues in the N-terminal extracellular domain of the $\alpha 7/5HT_3$ chimera that are $5HT_3$ sequence were switched to $\alpha 7$ sequence by QuickChange mutagenesis. The converse change was also made, using QuickChange mutagenesis, to the $\alpha 7$ nAChR clone in pRBG4 (i.e., the five residues in the N-terminal extracellular domain just to the N-terminal side of transmembrane region M1 were switched to $5HT_3$ sequence). The switched sequences were in the M2–M3 loop [DTLPATIGT ($5HT_3$) and EIMPATSDSV ($\alpha 7$)], at the C-terminal extracellular tail [HYS ($5HT_3$) and VEA VSKDFA ($\alpha 7$)] and in the N-terminal domain [IIRRR ($5HT_3$) and TMRRR ($\alpha 7$)].

Electrophysiology. *Xenopus* oocytes were isolated and maintained as described previously (10). In some cases, the oocytes were injected, as described previously (10), with

cRNA encoding human nAChR subunits; the cRNA was generated as described previously (11). The cDNA clones of human nAChR subunits that were used for making cRNA were from J. Garrett (Cognetix Inc., Salt Lake City, UT). For other experiments, plasmids carrying an $\alpha 7/5HT_3$ chimera, mutants of it, or a Q117S $\alpha 7$ nAChR mutant were introduced directly into the nuclei of the oocytes by injecting 4 ng of the DNA, in a volume of 10 nL, just below the very center of the dark hemispheres. The DNA was dissolved in 88 mM NaCl, 1 mM KCl, and 15 mM HEPES (pH 7). These plasmids have been described previously (9) or are outlined above.

A cylindrical 30 μ L oocyte bath made from Sylgard was gravity perfused with ND96A [96 mM NaCl, 2.0 mM KCl, 1.8 mM $CaCl_2$, 1.0 mM $MgCl_2$, 5 mM HEPES (pH 7.1–7.5), and 1 μ M atropine, all from Sigma (St. Louis, MO) or Research Organics (Cleveland, OH)]. The perfusion medium could be changed to one composed of ND96A and ACh (AChCl, Sigma) using a series of three-way solenoid valves.

Oocytes expressing the various receptors were maintained in the bath and were voltage clamped at -70 mV using a two-electrode voltage clamp (model OC-725B, Warner Instrument, Hamden, CT). Details of the voltage clamp apparatus have been described previously (10). Electrical currents through oocyte-expressed nAChRs were gated by pulses of ND96A containing ACh. Mostly, we used pulses that were 1 s in length and were 1 min apart; for $\alpha 1\beta 1\delta\epsilon$ channels, however, ACh was applied only once every 2 min to prevent receptor desensitization. For a given receptor, ACh was applied at close to the EC_{50} of activation (200 μ M for the human $\alpha 7$ receptor; 100 μ M for the rat $\alpha 3\beta 2$ receptor and human $\alpha 2\beta 2$, $\alpha 2\beta 4$, $\alpha 3\beta 2$, $\alpha 3\beta 4$, $\alpha 4\beta 2$, and $\alpha 4\beta 4$ receptors; 50 nM for the human $\alpha 1\beta 1\delta\epsilon$ receptor; 200 μ M for the $\alpha 7/5HT_3$ chimera and N111S chimera mutant; 50 mM for Y195T and W148T chimera mutants; and 10 mM for the Q117S chimera mutant and the Q117S $\alpha 7$ nAChR mutant). ACh-gated currents were electronically recorded as described previously (10). Millimolar concentrations of ACh had to be used on some $\alpha 7/5HT_3$ mutants (presumably because the mutations, in the ACh binding site, greatly reduced the potency of the agonist), and we thus made sure that the resulting large changes in ion concentration during the agonist pulses did not affect observed inhibition by the toxins. First, for the Y195T mutant, we showed that during 50 mM AChCl pulses, the transient increase in monovalent ions did not affect currents through the channel. This was done by applying 1 s test pulses of 50 mM *N*-methyl-D-glucamine chloride (NMDGCl), instead of 50 mM AChCl, in ND96; these pulses did not gate currents. We also showed that inhibition of the Y195T mutant was unaffected when the channel was gated with pulses of 50 mM AChCl in ND46A [46 mM NaCl, 2.0 mM KCl, 1.8 mM $CaCl_2$, 1.0 mM $MgCl_2$, 5 mM HEPES (pH 7.1–7.5), and 1 μ M atropine] instead of 50 mM AChCl in ND96A (this was demonstrated at 10 and 100 μ M α -ImI and 10 and $10/3$ μ M α -ImII). To show that the transient reduction in the level of Na^+ during this control experiment had no effect on currents through the channel, we used 1 s test pulses with 50 mM NMDGCl, instead of 50 mM AChCl, in ND46A; these pulses did not gate currents. In a similar control on the W149T mutant, α -ImI (at 10 and 100 μ M) and α -ImII (at 10 and $10/3$ μ M) exhibited the same degree of inhibition of currents

gated by 50 mM ACh pulses in ND46A and 50 mM ACh in ND96A. Also, on the Q117S chimera mutant, the two toxins (at 0.01 and 0.1 μ M for α -ImI and 10^{-3} μ M for α -ImII) exhibited the same degree of inhibition of currents gated by 10 mM ACh in ND86A [86 mM NaCl, 2.0 mM KCl, 1.8 mM CaCl₂, 1.0 mM MgCl₂, 5 mM HEPES (pH 7.1–7.5), and 1 μ M atropine] and 10 mM ACh in ND96A.

To determine the concentration dependence of inhibition of nAChRs by α -ImI and α -ImII, the peptides were applied using a static bath method; i.e., the ACh pulses and ND96A flow were halted, and conotoxin was applied at various concentrations to the bath. After the toxins had been allowed to reach equilibrium with the receptors (see below), the flow of ND96A was resumed at the same time as an ACh pulse was applied. To determine the inhibition at different toxin concentrations, the peak current elicited by the first ACh pulse following toxin exposure was converted to a percentage of the peak current elicited in control experiments in which ND96A alone, instead of toxin, was applied. To ensure toxins were at equilibrium, inhibitions after 5 and 10 min applications were compared for all toxin–receptor combinations, and no differences were seen except for α -ImI on the Q117S chimera mutant and the Q117S α 7 receptor mutant. In these cases, there was no difference between 10 and 20 min toxin applications; therefore, 10 min toxin pre-equilibration was used.

Data were analyzed and plotted using Prism Software (GraphPad Software, San Diego, CA). The inhibition data were fit to the equation

$$\% \text{ response} = 100/[1 + ([\text{toxin}]/\text{IC}_{50})^{n_H}]$$

where n_H is the Hill coefficient.

α -ImI Docking. A structural model of the major extracellular domain of the human α 7 receptor (12), based on homology to the acetylcholine binding protein (12) and scanning lysine mutagenesis (13), was used as a binding site for molecular docking simulation (14). Partial atomic charges were assigned to each atom of two adjacent receptor subunits using the restrained electrostatic potential (RESP) charge model of AMBER 7 (15). The set of 20 NMR structures of α -ImI was downloaded from the Protein Data Bank (PDB entry 1IMI), and the RESP charge model was again applied in assigning partial atomic charges for each NMR structure. Docking simulation of α -ImI was carried out using AUTODOCK 3.0.3 (16), which uses the Lamarckian genetic algorithm, and grid sizes of $60 \times 60 \times 60$ (a grid spacing of 0.375 Å was used). Ten toxin–receptor complexes were produced for each NMR structure. From the resulting 200 ligand–receptor complexes, the one with the lowest binding energy was selected as the most probable orientation of α -ImI in the binding site. The resulting receptor–ligand complex was refined using the side chain rotamer library and energy minimization routines found in JACKAL 1.5 (obtained at <http://trantor.bioc.columbia.edu>) to yield the final docked structure. This was compared to independent double mutant cycles data showing pairs of residues that stabilize the complex between α -ImI and the α 7/5HT₃ chimeric receptor.

RESULTS

α -ImI and α -ImII Interact with Different α 7 nAChR Residues. α -ImI binds to the classical ligand binding site of

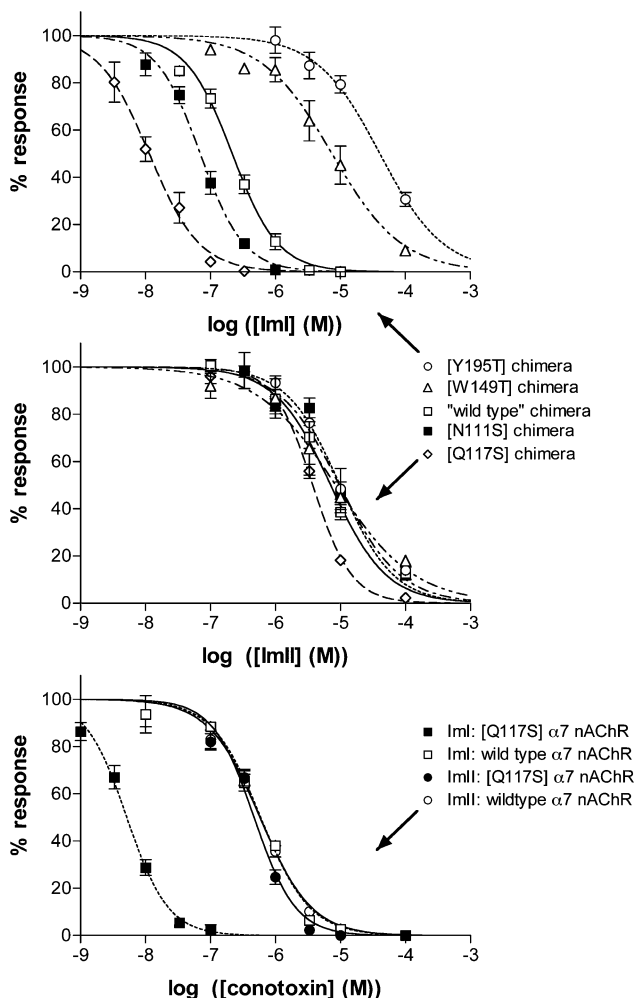


FIGURE 1: Inhibition of an α 7/5HT₃ chimera and various mutants of it by α -ImI (top) and α -ImII (middle) and inhibition of the α 7 nAChR and a Q117S mutant of it by α -ImI and α -ImII (bottom). The graphs show the concentration dependence of inhibition of peak currents, gated by 1 s ACh pulses, through the indicated receptors. The IC₅₀ values and Hill slopes of the best fit curves are given in Table 2. The line styles used for the best fit curves are the same in the two top graphs. Each point is the average of at least three measurements \pm the standard error of the mean.

the homomeric α 7 nAChR by interacting with residues on both the principal and complementary faces of the cleft between adjacent receptor subunits (9). To compare interactions of α -ImI and α -ImII with the α 7 nAChR, we used receptor mutants with changes at amino acids that have previously been implicated in contacts with α -ImI (9). The mutations were initially generated for earlier studies (8, 9) and were in the context of an α 7/5HT₃ chimera which is a model for the α 7 nAChR. The chimera has the extracellular, ACh-binding domain of the human α 7 nAChR in place of the equivalent portion of the highly homologous 5HT₃ receptor. This and similar chimeras have been widely used in studies of ligand binding because they are expressed at higher levels than the α 7 nAChR on the surfaces of mammalian cells. For α -ImI, the different mutant receptors showed the same rank order in the IC₅₀–mutant/IC₅₀–wildtype ratios determined by assessment of functional inhibition (Figure 1 and Table 2) and the K_{app} –mutant/ K_{app} –wildtype ratios determined via a competition binding assay (9). In contrast, α -ImII did not distinguish between the “wild-type” chimera

Table 2: IC₅₀ Values and Hill Slopes (n_H) for Inhibition of Wild-Type and Mutant $\alpha 7/5HT_3$ Chimeras by α -ImI and α -ImII^a

receptor	IC ₅₀ (95% confidence interval) ^b (μ M)	n_H (95% confidence interval)	IC _{50-mutant} /IC _{50-wildtype}	$K_{app-mutant}$ / $K_{app-wildtype}$ ^c
α -ImI				
wild-type chimera	0.217 (0.185–0.253)	1.23 (0.75–1.28)	NA ^d	NA ^d
Y195T chimera	40.7 (29.6–56.0)	0.89 (0.66–1.45)	188	328
W149T chimera	7.44 (5.46–10.1)	0.81 (0.57–1.05)	34.3	27.4
N111S chimera	0.0700 (0.0586–0.0836)	1.29 (0.98–1.60)	0.323	0.15
Q117S chimera	0.0143 (0.00890–0.0147)	1.12 (0.82–1.42)	0.0659	0.07
Q117S $\alpha 7$ nAChR	0.00517 (0.00448–0.00597)	1.36 (1.12–1.61)	0.0238 ^e	
α -ImII				
wild-type chimera	7.08 (5.63–8.89)	1.02 (0.75–1.28)	NA ^d	
Y195T chimera	9.88 (7.13–13.7)	1.06 (0.66–1.45)	1.40	
W149T chimera	8.43 (5.50–13.0)	0.72 (0.47–0.96)	1.19	
N111S chimera	9.68 (7.15–13.1)	0.94 (0.67–1.20)	1.37	
Q117S chimera	3.75 (3.40–4.14)	1.44 (1.23–1.66)	0.530	
Q117S $\alpha 7$ nAChR	0.469 (0.402–0.548)	1.36 (1.09–1.63)	0.821 ^e	

^a For both toxins, the IC_{50-mutant}/IC_{50-wildtype} ratio is shown for every mutant. For α -ImI, the $K_{app-mutant}$ / $K_{app-wildtype}$ ratio, previously determined with the competition binding assays (9), is also shown. ^b The 95% confidence interval. ^c K_{app} is the apparent dissociation constant determined in a previous study (9). ^d Not applicable. ^e The relevant wild-type IC₅₀ values are given in Table 4.

and the mutants; i.e., the IC_{50-mutant}/IC_{50-wildtype} ratios were close to unity (Figure 1 and Table 2).

α -ImII exhibited a slight (2-fold) increase in potency for the Q117S chimera mutant; however, this is much less than the corresponding 15-fold increase in α -ImI potency, and it was not seen for a Q117S mutation in the context of the native $\alpha 7$ nAChR (Figure 1, bottom panel, and Table 2). This small effect may thus be due to the higher concentrations of α -ImII that are needed to inhibit the $\alpha 7/5HT_3$ chimera (see below), and it suggests a minor low-affinity inhibitory interaction between α -ImII and the residue at position 117. Because none of the mutations at residues that interact with α -ImI strongly affect α -ImII, we conclude that the toxins have very distinct binding determinants.

α -ImI Binding Site Revealed by Computational Docking. To better understand the structural basis of the high affinity of α -ImI binding, and by contrast the inability of α -ImII to bind at the α -ImI site, we generated a structural model of the $\alpha 7$ nAChR with bound α -ImI. We used a homology model of the ligand binding domain of the $\alpha 7$ receptor (14) and a set of published NMR structures of α -ImI (17). The modeling was independent of functional inhibition and competition binding measurements. Computational docking yielded a single, energetically preferred structural model of the complex (see Materials and Methods and Figure 2). The model predicts that α -ImI docks at the cleft formed at the interface between $\alpha 7$ nAChR subunits with its disulfide bridges facing peripherally and side chains penetrating into the binding site. Consistent with previous mutant cycle analysis (9) and the functional data outlined above, α -ImI makes contacts at both the principal and complementary faces. Arg7 of α -ImI is anchored to the principal face via its guanidinium moiety, which is surrounded by the aromatic rings of Y195, W149, and Y92 of the receptor (Table 3). Trp10 of α -ImI penetrates deep into the cleft and provides a secondary anchor by closely contacting T77 and N111 of the complementary face. Also consistent with the functional data given above, and previous identification of residues that affect α -ImI binding affinity (9), the model shows that Q117 of the complementary face is close to Pro6 of α -ImI and probably interacts with the toxin.

Assuming that α -ImI and α -ImII have similar backbone structures, the two Arg residues of α -ImII that replace Pro6

and Ala9 of α -ImI will place additional bulk and two more positive charges on the side of the toxin that faces the complementary face of the binding site. Both the additional charges and steric bulk may prevent α -ImII from fitting into the α -ImI binding cleft. Loss of conformational rigidity in α -ImII, due to the replacement of Pro6 with Arg, might also make α -ImII incompatible with the simultaneous contacts at the principal and complementary faces that stabilize α -ImI binding.

Differential Potency of α -ImII on the $\alpha 7$ nAChR and an $\alpha 7/5HT_3$ Chimera. During characterization of the wild-type $\alpha 7/5HT_3$ chimera, we made the surprising observation that the IC₅₀ of α -ImII is ~ 12 -fold greater for the chimera than for the $\alpha 7$ nAChR (7.08 μ M vs 571 nM), whereas the IC₅₀ of α -ImI for the chimera (217 nM) was similar to its IC₅₀ for the $\alpha 7$ nAChR (595 nM). Thus, the presence of 5HT₃ sequence in the membrane-spanning domains and intervening linkers of the chimera has little effect on functional antagonism by α -ImI but significantly impairs antagonism by α -ImII.

Given this observation, we postulated that the α -ImII binding site might consist of extracellular portions of the $\alpha 7$ nAChR that are replaced by 5HT₃ sequence in the chimera, thus disrupting α -ImII binding. However, mutational analysis of extracellular portions of the $\alpha 7$ nAChR and the $\alpha 7/5HT_3$ chimera did not support this model. Three putative non- $\alpha 7$ extracellular regions of the chimera were investigated: (1) the extracellular loop between transmembrane regions M2 and M3, (2) the C-terminal extracellular tail, and (3) the five residues in the N-terminal extracellular domain that are just to the N-terminal side of transmembrane region M1. We found that conversion of the loop, the tail, and both simultaneously, from 5HT₃ sequence to $\alpha 7$ sequence in the chimera, did not increase the potency of α -ImII inhibition (data not shown). Also, the five residues in the N-terminal extracellular domain of the $\alpha 7$ nAChR that are replaced with 5HT₃ sequence in the chimera do not appear to interact with α -ImI; conversion of this region to 5HT₃ sequence in the context of the $\alpha 7$ nAChR did not reduce the potency of α -ImII for the receptor (data not shown). (Mutation of this region to $\alpha 7$ sequence in the context of the chimera did not give functional channels.) Thus, the decrease in α -ImII potency for the chimera is not due to

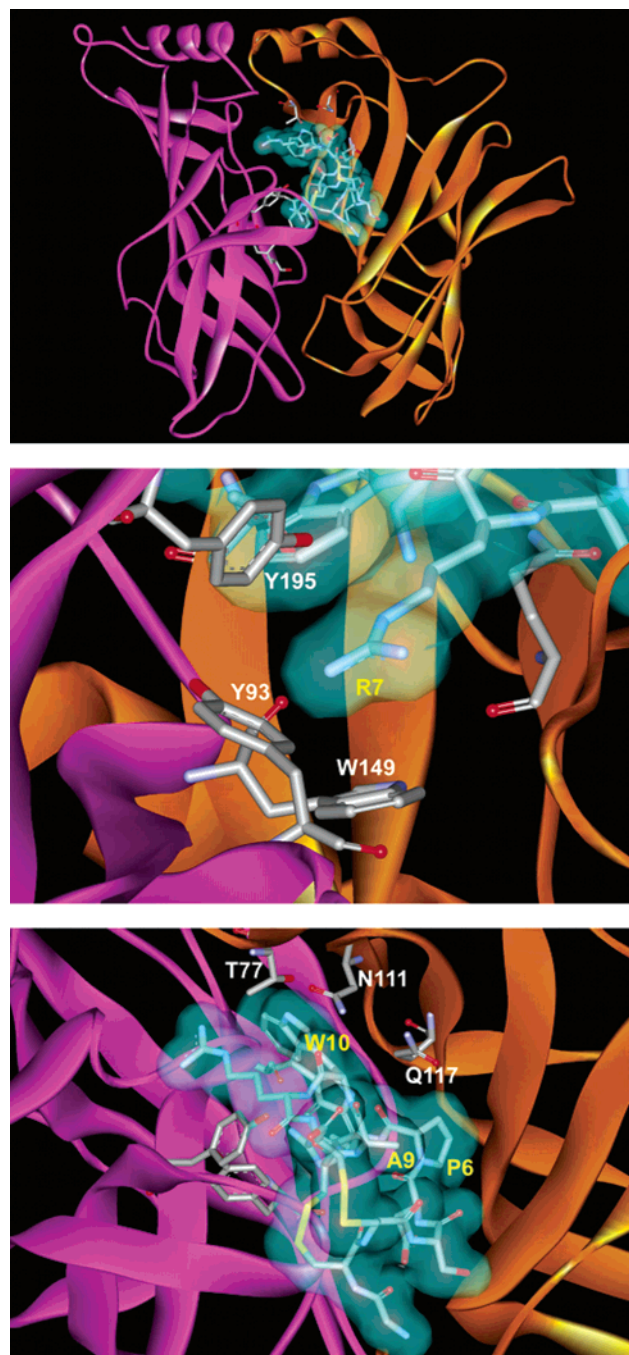


FIGURE 2: Complex between α -conotoxin ImI and $\alpha 7$ nAChR determined by computational docking. The top panel shows the overall complex with the principal face of the binding site highlighted in magenta and the complementary face in orange. Receptor subunits are rendered as secondary structures, with side chains of key binding site residues in stick representation. The van der Waals surface is superimposed over a stick representation of α -ImI. The middle panel shows a close-up view of Arg7 of α -ImI surrounded by aromatic residues from the principal face of the binding site. The bottom panel shows a close-up of contacts between α -ImI and the complementary face of the subunit. In all three panels, the complex is displayed in roughly the same orientation.

replacement of $\alpha 7$ sequence with 5HT₃ sequence at the predicted extracellular sites. Other possibilities are that α -ImII may interact with the ion-conducting pore of the receptor, or a region of the N-terminal extracellular domain that is allosterically disrupted in the chimera.

Inhibition Profiles of Different nAChR Subtypes by α -Conotoxins ImI and ImII. The inhibition of peak currents gated

Table 3: Distances between Residues of α -ImI and the $\alpha 7$ nAChR^a

toxin residue	$\alpha 7$ nAChR residue	distance (Å)
D5	Y195	10.7
D5	W149	11.1
D5	Y93	14.5
D5	W55	6.5
P6	Q117	3.7
R7	Y195	3.9
R7	W149	4.2
R7	Y92	6.3
R7	Y188	6.3
R7	W55	3.6
A9	Q117	5.6
W10	T77	2.3
W10	N111	4.4
W10	Q117	8.1

^a The distances are the closest approaches between heavy atoms in the side chains of both members of a pair.

by 1 s ACh pulses was measured for seven different human neuronal nAChR subtypes expressed in *Xenopus* oocytes (see Figure 3 and Table 4). α -ImI and α -ImII were seen to have distinct potency profiles; α -ImI was most potent against the human $\alpha 3\beta 2$ nAChR, whereas α -ImII was most potent against the human $\alpha 7$ receptor. In addition, the two peptides were tested on oocytes expressing the human muscle subtype $\alpha 1\beta 1\delta \epsilon$. α -ImII was an inhibitor of this receptor, but α -ImI was not.

DISCUSSION

Conotoxin α -ImI binds at the classical ligand site of the homomeric $\alpha 7$ nAChR by interacting with residues on the principal and complementary faces of adjacent receptor subunits, i.e., in the cleft between adjacent subunits (9). A previous study (6) showed that the sequence of another $\alpha 4/3$ -conotoxin, α -ImII, is 75% identical to that of α -ImI and, like α -ImI, α -ImII inhibits the rat $\alpha 7$ receptor; however, it appears to bind a different site on the receptor. This conclusion was based on competition studies: only α -ImI competes with α -bungarotoxin for binding to the receptor, and α -ImI and α -ImII do not compete with each other for binding. In this study, we used oocyte electrophysiology to show that α -ImII does not interact with residues of the human $\alpha 7$ receptor that interact with α -ImI.

On the basis of previously published data (9) and the docking model outlined in the Results, we selected amino acid mutations that are diagnostic for the α -ImI binding site (Y195T, W149T, N111S, and Q117S). These mutations alter residues that are implicated in interactions with α -ImI (9) and that are located on opposite sides of the α -ImI binding site: W149 and Y195 on the principal face and N111 and Q117 on the complementary face. Thus, collectively, these mutations are expected to disrupt many toxin–receptor interactions from widely spaced parts of the α -ImI binding site, and they significantly define the region of contact involved in α -ImI binding. Since α -ImII does not compete with α -bungarotoxin, there is no known binding assay available for this peptide, and therefore, the mutations that we selected had to be able to be functionally expressed in *Xenopus* oocytes. As a result, some $\alpha 7$ receptor residues previously shown to interact with α -ImI could not be evaluated in this study; e.g., T77K $\alpha 7/5HT_3$ has a reduced affinity for α -ImI (9), but when we expressed it in oocytes,

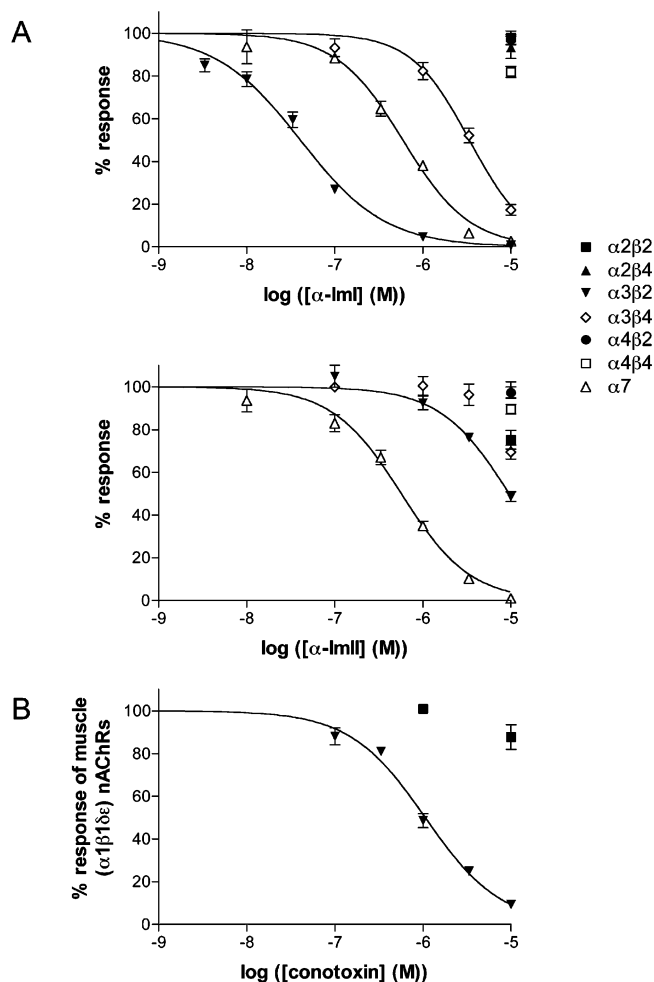


FIGURE 3: (A) Inhibition of human neuronal nAChR subtypes by α -ImI (top) and α -ImII (bottom). The graphs show the concentration dependence of inhibition of peak currents, gated by 1 s ACh pulses through the indicated nAChR subtypes. Best fit curves have been determined in some cases, and the corresponding IC_{50} values and Hill slopes are given in Table 4. (B) Inhibition of the adult human muscle nAChR subtype by α -ImI and α -ImII. The graph shows the concentration dependence of inhibition of peak currents through human $\alpha 1\beta 1\delta\epsilon$ nAChRs that were gated by 1 s pulses of ACh. The α -ImI data are represented by squares and the α -ImII data by triangles. The IC_{50} value and Hill slope from the best fit curve are given in Table 4. Each point is the average of at least three measurements \pm the standard error of the mean.

Table 4: IC_{50} Values and Hill Slopes (n_H) for Inhibition, by α -ImI and α -ImII, of Human nAChRs

human nAChR subtype	IC_{50} (95% confidence interval ^a), n_H (95% confidence interval)	
	α -ImI	α -ImII
$\alpha 2\beta 2$	> 10 μ M, ND ^b	> 10 μ M, ND
$\alpha 2\beta 4$	> 10 μ M, ND	> 10 μ M, ND
$\alpha 3\beta 2$	40.8 nM (35.8–47.8 nM), 0.90 (0.77–1.03)	9.61 μ M (8.33–1.11 μ M), 1.10 (0.91–1.29)
$\alpha 3\beta 4$	3.39 μ M (2.91–3.94 μ M), 1.32 (1.03–1.60)	> 10 μ M, ND
$\alpha 4\beta 2$	> 10 μ M, ND	> 10 μ M, ND
$\alpha 4\beta 4$	> 10 μ M, ND	> 10 μ M, ND
$\alpha 7$	595 nM (523–676 nM), 1.15 (0.97–1.33)	571 nM (501–652 nM), 1.11 (0.93–1.29)
muscle ($\alpha 1\beta 1\delta\epsilon$)	> 10 μ M, ND	1.06 μ M (9.38–1.21 μ M), 1.02 (0.89–1.14)

^a The 95% confidence interval. ^b Not determined.

ligand-gated currents could not be elicited even by high ACh concentrations (> 50 mM).

As expected, the Y195T, W149T, N111S, and Q117S mutations strongly affected the potency of α -ImI for the receptor. This is consistent with our docking analysis because the four mutated residues closely approach α -ImI in the structural model. Consistent with previous competition binding data, (9) the rank order of α -ImI potency for the mutants was as follows: Q117S > N111S > wild type > W148T > Y195T. In contrast, the mutations had a minimal effect on functional inhibition by α -ImII, showing that α -ImI and α -ImII have very different binding determinants on the human $\alpha 7$ receptor. Since α -ImI binds to this receptor by interacting with residues in regions that make up the ACh binding site (8, 9), the data indicate that the α -ImII binding site does not overlap with either the ACh or α -ImI site and that α -ImII, unlike α -ImI, is probably a noncompetitive inhibitor.

To understand the structural basis for the effects of the mutations on α -ImI potency, we generated a structural model of α -ImI bound to the $\alpha 7$ nAChR. Although the modeling employed rigid body docking for each complex, flexibility of α -ImI was incorporated because complexes were generated for each of 20 published NMR structures, one of which yielded the lowest binding energy. The model in Figure 2 reveals a close association between Arg7 of α -ImI and the side chains of the principal face residues Y195, W149, and Y93 (see Table 3). This close association strongly suggests a cation– π interaction between the guanidinium of Arg7 and these aromatic side chains. These principal face contacts are consistent with our functional data showing that α -ImI has reduced potency for the Y195T and W149T mutants and the previous observation that Y195, W149, and Y93 interact with Arg7 of α -ImI (9). Figure 2 and Table 3 reveal a close juxtaposition of Trp10 of α -ImI with T77 and N111 on the complementary face. This agrees with our observation that the N111S mutation alters the potency of inhibition by α -ImI and previous mutant cycle analysis (9), indicating that both T77 and N111 interact with Trp10 of α -ImI. The model of the complex also reveals that Q117 of the receptor is close to Pro6 of α -ImI and is likely to interact with the toxin; again, this is consistent with the functional data which show that the Q117S mutation alters the potency of inhibition by α -ImI, and previous data (9) showing that the affinity of α -ImI for the receptor is significantly affected by mutations at this residue.

In contrast, the docking model indicates that Asp5 of α -ImI is far from Y195 of the receptor (Table 3) despite double mutant cycle data that suggest interaction between these residues (9). This discrepancy could be explained if the experimentally revealed D5–W149 interaction is not direct and is a consequence of conformational changes in α -ImI resulting from the D5N mutation used in the mutant cycle analysis; specifically, replacement of Asp5 with Asn will remove a negative charge within 5 Å of the positively charged amino terminus (Figure 2), and the resulting loss of electrostatic attraction may change the conformation of α -ImI, thus indirectly disrupting interaction with W149.

While this paper was being reviewed, an alternative model of α -ImI docked to the $\alpha 7$ ligand binding domain appeared (18). The docking simulation that was used was different from ours since distance constraints based on experimentally determined pairwise interactions (9) were incorporated, a different structural model of the $\alpha 7$ ligand binding domain

was used, and a different docking program was employed. Like we do (Table 3), Dutertre et al. show close association between R7 of α -ImI and the receptor residues Y195 and W149, as well as juxtaposition of W10 of α -ImI and receptor residues N111 and T77. As in our docking analysis, the Dutertre model shows Q117 of the receptor to be proximal to bound α -ImI; however, our structure has the Q117 proximal to P6 of the toxin, whereas Dutertre et al. show it close to A9. Also, our model shows that D5 of α -ImI is far from W149 and Y195, but the Dutertre model suggests close association, presumably because pairwise interactions between these residues were used to constrain this model. Thus, as discussed above, we attribute the D5–W149 interaction revealed by mutant cycles analysis to indirect effects. The docking model of α -ImI described here has some features in common with that of Dutertre et al., but it also shows significant differences.

Our model of the $\alpha 7$ receptor bound to α -ImI suggests two possible reasons why α -ImII has negligible affinity for the α -ImI site. First, assuming α -ImII has the same backbone structure as α -ImI, substitution of two Arg residues in α -ImII will add positive charges and steric bulk that would have to be accommodated by the complementary face of the binding site. Another reason α -ImII may not bind at the α -ImI site involves the Pro6 to Arg6 change between α -ImI and α -ImII. Arg6 of α -ImII removes the restriction of the backbone ϕ angle imposed by Pro6 in α -ImI, potentially producing widespread conformational differences between α -ImI and α -ImII. Such differences could make the relative positions and orientations of Arg7 and Trp10 of α -ImII incompatible with the simultaneous principal and complementary face interactions that our structural model and previous data (9) reveal to be necessary for α -ImI binding. The importance of Pro6 in determining the three-dimensional structure of α -ImI is suggested by its potential involvement in forming the distorted helix between Asp5 and Arg10 of this toxin (17). However, the two disulfide bridges also help create this helicity, and CD spectra of wild-type, P6A, and P6S α -ImI do not indicate dramatic differences in the secondary structural elements that are present (19). Therefore, while extensive structural differences between α -ImI and α -ImII cannot be ruled out, they are unlikely.

Previous mutagenesis data support our suggestion that Arg at position 6 of α -ImII is incompatible with binding at the α -ImI site. It has been shown that a mutant version of α -ImI in which Pro6 is replaced with Arg does not compete with α -bungarotoxin, whereas native α -ImI can (6).

An additional difference between the toxins is that α -ImI inhibits the $\alpha 7$ nAChR and the $\alpha 7/5HT_3$ chimera with similar potencies, but α -ImII has 12-fold less potency for the chimera (Tables 2 and 4). This difference further supports the conclusion that the two toxins have distinct binding sites; it suggests that the α -ImII site is disrupted in the context of the $\alpha 7/5HT_3$ chimera whereas the α -ImI site is not. We postulated that this might be because α -ImII binds to extracellular parts of the $\alpha 7$ nAChR that, in the context of the $\alpha 7/5HT_3$ chimera, no longer consist of $\alpha 7$ sequence and are thus changed relative to the native receptor. However, as outlined in the Results, mutagenesis of the $\alpha 7$ nAChR and the $\alpha 7/5HT_3$ chimera did not support this model; an alternative possibility is that α -ImII binds to the N-terminal extracellular domain at a site that is allosterically disrupted

by the presence of 5HT₃ sequence in the chimera. A second possibility is that α -ImII interacts with the ion-conducting channel of the $\alpha 7$ nAChR, although, because α -ImII does not seem to be an open channel blocker (6), the toxin probably does not bind to regions of the channel that are only accessible when the channel is open.

We also examined the subtype specificity of α -ImI and α -ImII on a range of human neuronal nAChRs ($\alpha 7$, $\alpha 2\beta 2$, $\alpha 2\beta 4$, $\alpha 3\beta 2$, $\alpha 3\beta 4$, $\alpha 4\beta 2$, and $\alpha 4\beta 4$) and a human muscle subtype ($\alpha 1\beta 1\delta\epsilon$). In this screening, we measured the ability of the toxins to reduce maximum currents gated by 1 s pulses of ACh. As shown in Figure 3, of the human neuronal nAChR subtypes that have been tested, α -ImI was most potent against the $\alpha 3\beta 2$ receptor. This was surprising because α -ImI was previously seen to have no effect, at 5 μ M, on rat $\alpha 3\beta 2$ channels (20). In our hands, α -ImI also strongly inhibited the rat $\alpha 3\beta 2$ nAChR (70% block at 1 μ M). In contrast to α -ImI, α -ImII was most potent against the $\alpha 7$ receptor. In addition, α -ImII was found to be a potent inhibitor of the $\alpha 1\beta 1\delta\epsilon$ subtype, whereas α -ImI was not. Since α -ImI and α -ImII bind different sites on the $\alpha 7$ nAChR, their different potencies against other nAChRs likely result from differences in these sites among receptor subtypes.

The overall data show that α -ImII interacts with a region of the $\alpha 7$ nAChR that is different from that which interacts with α -ImI, and that this region is changed in the context of the $\alpha 7/5HT_3$ chimera. It thus is a probe for an antagonist site that is distinct from the well-characterized α -ImI site which overlaps the classical ligand binding site of the receptor (21).

ACKNOWLEDGMENT

We Thank Sean Christensen and Brian Fiedler for oocyte preparation.

REFERENCES

- Paterson, D., and Nordberg, A. (2000) Neuronal nicotinic receptors in the human brain, *Prog. Neurobiol.* 61, 75–111.
- Maricq, A. V., Peterson, A. S., Brake, A. J., Myers, R. M., and Julius, D. (1991) Primary structure and functional expression of the 5HT₃ receptor, a serotonin-gated ion channel, *Science* 254, 432–437.
- Eiselé, J.-L., Bertrand, S., Galzi, J.-L., Devillers-Thiery, A., Changeux, J.-P., and Bertrand, D. (1993) Chimaeric nicotinic-serotonergic receptor combines distinct ligand binding and channel specificities, *Nature* 366, 479–483.
- McIntosh, J. M., Santos, A. D., and Olivera, B. M. (1999) Conus peptides targeted to specific nicotinic acetylcholine receptor subtypes, *Annu. Rev. Biochem.* 68, 59–88.
- McIntosh, J. M., Yoshikami, D., Mahe, E., Nielsen, D. B., Rivier, J. E., Gray, W. R., and Olivera, B. M. (1994) A nicotinic acetylcholine receptor ligand of unique specificity, α -conotoxin ImI, *J. Biol. Chem.* 269, 16733–16739.
- Ellison, M., McIntosh, J. M., and Olivera, B. M. (2003) α -Conotoxins ImI and ImII: Similar $\alpha 7$ nicotinic receptor antagonists act at different sites, *J. Biol. Chem.* 278, 757–764.
- Luo, S., Nguyen, T. A., Cartier, G. E., Olivera, B. M., Yoshikami, D., and McIntosh, J. M. (1999) Single-residue alteration in α -conotoxin PnIA switches its nAChR subtype selectivity, *Biochemistry* 38, 14542–14548.
- Quiram, P. A., and Sine, S. M. (1998) Structural elements in α -conotoxin ImI essential for binding to neuronal $\alpha 7$ receptors, *J. Biol. Chem.* 273, 11007–11011.
- Quiram, P. A., Jones, J. J., and Sine, S. M. (1999) Pairwise interactions between neuronal $\alpha 7$ acetylcholine receptors and α -conotoxin ImI, *J. Biol. Chem.* 274, 19517–19524.

10. Cartier, G. E., Yoshikami, D., Gray, W. R., Luo, S., Olivera, B. M., and McIntosh, J. M. (1996) A new α -conotoxin which targets $\alpha 3\beta 2$ nicotinic acetylcholine receptors, *J. Biol. Chem.* **271**, 7522–7528.
11. McIntosh, J. M., Corpuz, G. P., Layer, R. T., Garrett, J. E., Wagstaff, J. D., Bulaj, G., Vyazovkina, A., Yoshikami, D., Cruz, L. J., and Olivera, B. M. (2000) Isolation and characterization of a novel *Conus* peptide with apparent antinociceptive activity, *J. Biol. Chem.* **275**, 32391–32397.
12. Brejc, K., van Dijk, W. J., Klaassen, R. V., Schuurmans, M., van Der Oost, J., Smit, A. B., and Sixma, T. K. (2001) Crystal structure of an ACh-binding protein reveals the ligand-binding domain of nicotinic receptors, *Nature* **411**, 269–276.
13. Sine, S. M., Wang, H.-L., and Bren, N. (2002) Lysine scanning mutagenesis delineates structure of nicotinic receptor ligand binding domain, *J. Biol. Chem.* **277**, 29210–29223.
14. Henchman, R. H., Wang, H.-L., Sine, S. M., Taylor, P., and McCammon, J. A. (2003) Asymmetric structural motions of the homomeric $\alpha 7$ nicotinic receptor ligand binding domain revealed by molecular dynamics simulation, *Biophys. J.* **85**, 3007–3018.
15. Pearlman, D. A., Case, D. A., Caldwell, J. W., Ross, W. R., Cheatham, T. E., III, DeBold, S., Ferguson, D., Seibel, G., and Kiollman, P. (1995) AMBER, a computer program for applying molecular mechanics, normal mode analysis, molecular dynamics and free energy calculations to elucidate the structures and energies of molecules, *Comput. Phys. Commun.* **91**, 1–41.
16. Morris, G. M., Goodsell, D. S., Huey, R., and Olson, A. J. (1996) Distributed automated docking of flexible ligands to proteins: Parallel applications of AutoDock 2.4, *J. Comput.-Aided Mol. Des.* **10**, 293–304.
17. Maslennikov, I. V., Shenkarev, Z. O., Zhmak, M. N., Ivanov, V. T., Methfessel, C., Testlin, V. I., and Arseniev, A. S. (1999) NMR spatial structure of α -conotoxin ImI reveals a common scaffold in snail and snake toxins recognizing neuronal nicotinic acetylcholine receptors, *FEBS Lett.* **444**, 275–280.
18. Dutertre, S., Nicke, A., Tyndall, J. D. A., and Lewis, R. J. (2004) Determination of α -conotoxin binding modes on neuronal nicotinic acetylcholine receptors, *J. Mol. Recognit.* **17**, 339–347.
19. Lamthanh, H., Jegou-Matheron, C., Servent, D., Menez, A., and Lancelin, J. M. (1999) Minimal conformation of the α -conotoxin ImI for the $\alpha 7$ neuronal nicotinic acetylcholine receptor recognition: Correlated CD, NMR and binding studies, *FEBS Lett.* **454**, 293–298.
20. Johnson, D. S., Martinez, J., Elgoyhen, A. B., Heinemann, S. F., and McIntosh, J. M. (1995) α -Conotoxin ImI exhibits subtype-specific nicotinic acetylcholine receptor blockade: Preferential inhibition of homomeric $\alpha 7$ and $\alpha 9$ receptors, *Mol. Pharmacol.* **48**, 194–199.
21. Sine, S. M. (2002) The nicotinic receptor ligand binding domain, *J. Neurobiol.* **3**, 431–446.

BI048918G